Structural and Magnetic Properties of Zn-Doped Magnetite Nanoparticles Obtained by Wet Chemical Method

Sergio Ferrari, Juan Carlos Aphesteguy, and Fabio Daniel Saccone

Facultad de Ciencias Exactas y Naturales, Instituto de Tecnología y Ciencias de la Ingeniería Ing. Hilario Fernández Long, National Scientific and Technical Research Council, Buenos Aires, Argentina

The structural and magnetic properties of $Fe_{(3-x)}Zn_xO_4$ (x : 0, 0.1, 0.2, 0.5, 1) nanoparticles, prepared by wet chemical method, have been studied by X-ray diffraction (XRD), scanning electron microscopy (SEM), Mössbauer spectroscopy, and magnetization measurements. The nanoparticles are polyhedrical-shaped with a narrow distribution in size as it was verified by SEM. By Rietveld analysis of XRD patterns, it was determined that the crystallites' sizes of $Fe_{(3-x)}Zn_xO_4$ in spinel structure is in the range of 30 to 50 nm. Hysteresis cycles, measured at different temperatures (300, 200, 100, 50, and 7 K), showed an increase in saturation, while temperature is diminished, as it is expected. All the samples, exhibited a high blocking temperature of ∼350 K, as it was determined by ZFC-FC measurements. This fact, reveals their strongly interacting superparamagnetic nature. Real ac susceptibility increases with temperature, while the imaginary part has a maximum, which depends on frequency, and it is related to a critical temperature, which depends on composition. A Néel–Arrhenius dependence of frequency on the critical temperature was found for all the samples. We determined a minimum of the effective anisotropy for $x = 0.2$.

***Index Terms*— Magnetic nanoparticles, Zn-doped magnetite.**

I. Introduction

THE development of nanosized magnetic materials is a subject of considerable interest both for understanding their fundamental properties and for new technological applications because nanoparticles show unusual phenomena compared with bulk or microscale-sized magnets of the same composition [1]–[3].

Several magnetic and mixed metal oxides nanoparticles, having the general formula XY_2O_4, have been investigated because they exhibit interesting and unique physical properties in different areas, such as high density storage [4], color imaging, sensors, biomedical and biological applications [5], [6], spintronic [7], and catalysis.

In these oxidic spinels, the physical properties were found to be dependent on the nature of the involved ions, their charges, and their site distribution among 8-tetrahedral (A) and 16-octahedral (B) sites. Two extreme distributions of cations are possible: 1) the normal $(X)_A[Y_2]_BO_4$ and 2) the inverse $(Y)_A[XY]_BO_4$ distribution [8], where the ions in the octahedral sites are in square brackets. Blasse [9] and Behdadfar *et al.* [10] have studied solid solutions by substituting ions at A and B sites. They have obtained a gradual change in the physical and magnetic properties of these oxidic spinels by varying the composition of the solution.

Magnetite (Fe_3O_4) possesses an inverse spinel structure, where oxygen ions forms an fcc close packing, with a cation distribution after the formula $(Fe^{3+})_A[Fe^{2+}Fe^{3+}]_BO_4$, and is a ferromagnetic oxide with a Curie temperature at 858 K [11]. It has been found [12]–[14] that for substituted magnetite $M_xFe_{3-x}O_4$ (M = Zn, Mn), a fast electron exchange between Fe^{2+} and Fe^{3+} ions on octahedral sites in the spinel lattice is considered as the reason for the higher electrical conductivity in the case of lower values of x. For higher values, other conduction mechanisms should be considered. In addition, doping magnetite with transition elements allows the modification of quantities such as M_S. In addition, ferrimagnetic iron oxides have the largest M_S of all the known biocompatible materials and they are low cost.

Bulk zinc ferrite has a normal spinel structure with the diamagnetic Zn^{2+} ions in the tetrahedral sites and magnetic Fe^{3+} ions in the octahedral sites [15]. Due to antiferromagnetic superexchange interactions between octahedral-coordinated Fe^{3+} ions, bulk zinc ferrite is antiferromagnetic at $T_N = 10$ K. However, scaling to nanometer sizes the magnetic structure of zinc ferrites changes significantly with the redistribution of iron and zinc cations into octahedral and tetrahedral sites. As a result of nanometer scaling, nanocrystalline zinc ferrite shows ferromagnetic behavior. It has been demonstrated that the properties of zinc ferrites are strongly influenced by the composition and microstructure, and can be modified controllably by varying the particle size, processing parameters, and type and concentration of dopant [16]–[18]. Magnetic dilution due to substitution of diamagnetic atoms gives rise to interesting magnetic features in spinel structure compounds.

The aim of this paper is to identify the doping effect of Zn at different concentrations and to analyze its role on modifications of structure, morphology, and magnetic properties of Zn-doped magnetite. Magnetite sample and zinc-substituted samples were obtained by coprecipitation method for its advantage, such as easy preparation, enough digestion to form the final structure suitable, control of particle size, and low cost. We have studied the $Zn_xFe_{3-x}O_4$ system using X-ray diffraction (XRD), scanning electron microscopy (SEM), Mössbauer spectroscopy at room temperature (RT), FC-ZFC measurements, hysteresis loops at different

Manuscript received July 19, 2014; revised September 6, 2014 and October 20, 2014; accepted November 24, 2014. Corresponding author: F. D. Saccone (e-mail: fsaccone@fi.uba.ar).

Color versions of one or more of the figures in this paper are available online at http://ieeexplore.ieee.org.

Digital Object Identifier 10.1109/TMAG.2014.2377132

temperatures, and ac magnetic susceptibility measurements at different frequencies.

II. Experimental

A. Sample Preparation

Fe_3O_4 pure nanoparticles, Zn-doped ferrites according to the formula $Zn_xFe_{3-x}O_4$ with $x = 0.1$, 0.15, 0.2, and 0.5 were prepared by coprecipitation method in aqueous solution of iron sulfate and water mixed with a solution of KNO_3 and NH_3 (more details are given in Section II-A1). $ZnFe_2O_4$ powders were obtained by sol-gel method following a similar procedure employed in [19]. This last method was preferred for this sample, due to its preservation of stoichiometry as it inhibits the Fe^{2+} to Fe^{3+} oxidation.

1) Preparation of Undoped and Doped Magnetite: To prepare the pure and Zn-doped magnetite samples, N_2 was bubbled independently during 20 min through two solutions: 1) Solution 1: 50 mL of concentrated ammonia and KNO_3 (oxidant agent) with a concentration of 2×10^{-2} mol/L were completely dissolved in 540 mL of distilled water at RT and 2) Solution 2: 1.57×10^{-2} mol/L $FeSO_4 \cdot 7H_2O$ was dissolved in 6 mL of H_2SO_4 2M and 54 mL of distilled water at RT. After 20 min, Solution 2 was added slowly under vigorous mechanical stirring and flowing N_2 to Solution 1 at RT. Then the sample was kept at rest inside the reaction vessel at RT during 20 h in order to promote the complete formation of the spinel phase ($pH_{final} \approx 10.0$). The precipitates were separated from the slurry by centrifuging and washed several times with distilled water, methanol and acetone being finally pH $\approx$ 6. As the last step, the nanoparticles were dried in air. For Zn-doped samples $FeSO_4 \cdot 7H_2O$ was partially replaced by $ZnSO_4 \cdot 7H_2O$, in a fraction corresponding to the desired composition.

2) Zinc Ferrite Preparation: In order to prepare Zn ferrite, 0.01 mol $Zn(Ac)_2 \cdot 2H_2O$ and 0.02 mol $Fe(NO_3)_3 \cdot 9H_2O$ were dissolved in 50 mL of distilled water in a reaction vessel and were gelated using 0.1 mol citric acid as a catalyst. The solution was heated at 90 °C with continuous stirring until a highly viscous gel was formed. Then, the resulting gel was dried at 120 °C for 24 h in an oven.

B. Measurement Conditions

XRD was carried out by a Rigaku D/max diffractometer equipped with a vertical goniometer, using a Bragg–Ventano geometry ($\theta - 2\theta$ coupled arms) and Cu-Kα radiation in a $15°-80°$ 2θ range, measuring at every 0.05° step sweeping with a 0.5° per minute velocity. Microscopy images where captured with a Carl Zeiss SMT Supra 40 SEM at 3 kV. The Mössbauer measurements were recorded at RT under transmission geometry with a standard constant acceleration spectrometer, using a 5 mCi ^{57}CoRh radioactive source. Data was recorded using a 1024 channel MDAQ107 data acquisition module [20]. Magnetic properties were measured by a Quantum Design PPMS 9 T, applying a maximum field of 3 T in hysteresis loops. AC susceptibility was measured with frequencies of 107, 1007, 5007, and 9967 Hz applying 238.7 A/m magnetic field amplitude and sweeping temperatures between 5 and 300 K with a step of 5 K.

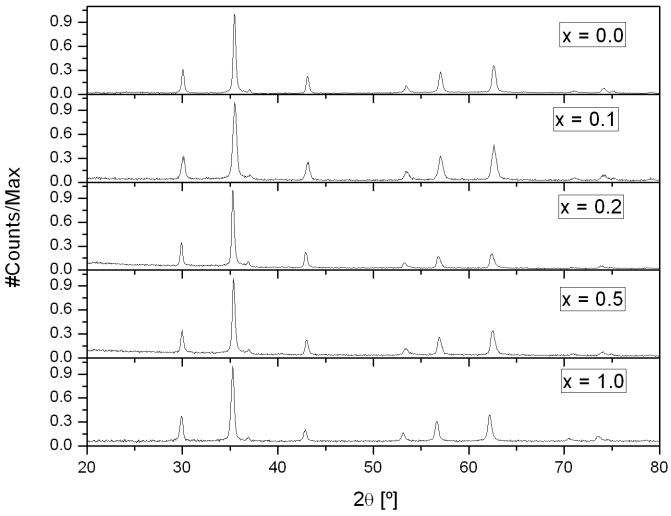

Fig. 1. XRD patterns for the different samples. From top to bottom: increasing zinc content referred in the value of x.

III. Results and Discussion

A. XRD, SEM Images, and Mössbauer Data

All XRD patterns on Fig. 1 shows the typical peaks of magnetite cubic structure (space group Fd3m) with no observation of extra ones which indicate, in principle, that no segregation of other crystalline phases was induced during the synthesis. Then, Zn was incorporated as a dopant, as it was expected. By a Rietveld analysis of the patterns, we estimated the lattice constant between 8.39 and 8.41 Å, and an average grain size in all samples of 45 nm. In details, pure magnetite showed the highest grain size of 55 nm, while for $x = 0.1$ we found the lowest grain size of ~34 nm.

SEM images of synthesized nanoparticles samples with $x = 0$ and $x = 0.1$ are shown in Fig. 2. As it can be seen, the nanoparticles are polyhedrical-shaped with a narrow distribution in size. The observed nanoparticle diameters are larger than the mean grain size as obtained by Rietveld refinement analysis of diffraction patterns. This can be explained from the fact that Rietveld analysis give us information about crystallite sizes rather than the nanoparticle diameter. On the other hand, the mean nanoparticle diameter for $x = 0.1$ is larger than that for $x = 0$. These differences with the results determined by Rietveld analysis for the crystallite size seems to be related to a higher nanoparticles coalescence for $x = 0.1$ than for $x = 0$.

Mössbauer spectroscopy (Fig. 3) showed that partial Zn dilution promotes a higher disorder degree preferentially in the octahedral site (see spectra for samples with $x = 0$, 0.1, 0.2, and 0.5). For $x = 0$ and for $x = 0.1$, we found the evidence of three non-equivalent sites for the ^{57}Fe probe (we fitted its corresponding spectrum with two magnetic sextets, corresponding to tetrahedral sites (A) and octahedral (B) sites, and a quadrupolar interaction (QI). The hyperfine parameters corresponding to octahedral sites (Table I) and its broadened linewidth show that they are occupied by iron probes with a mixed valence between

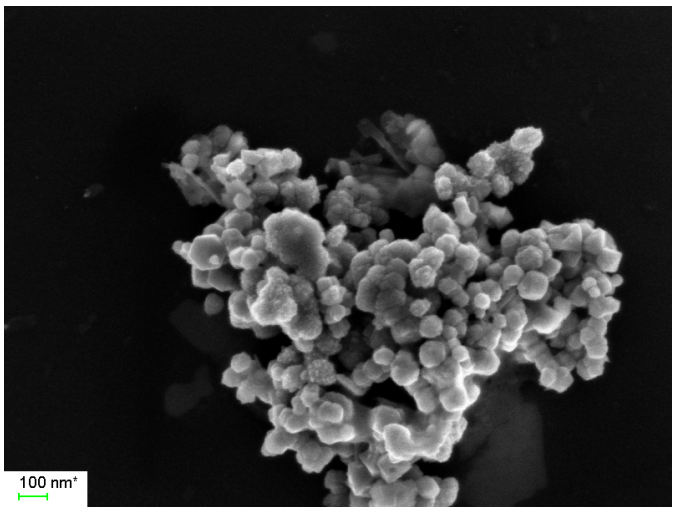

(a)

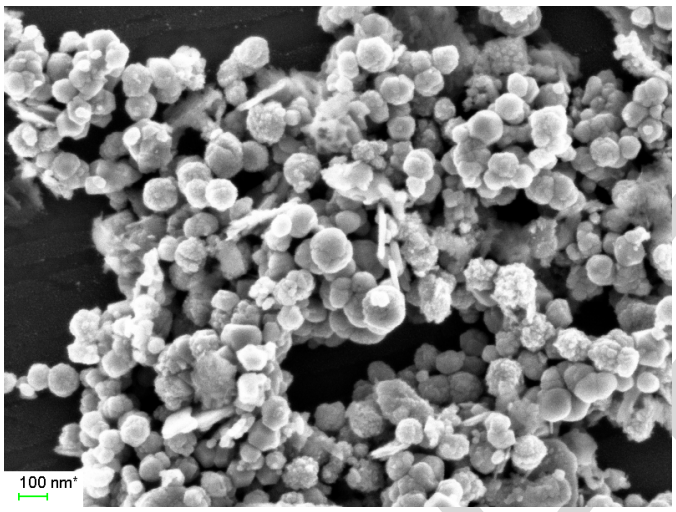

(b)

Fig. 2. SEM images of samples with (a) $x = 0$ and (b) $x = 0.1$.

Fe^{2+} and Fe^{3+} [21]. For the other two above-mentioned concentrations ($x = 0.2$ and $x = 0.5$), it was necessary to add an additional sextet in order to reproduce the presence of a more distorted environment. This additional sextet has a lower hyperfine magnetic field (~40 T) and is assumed that it shows a different neighborhood for ^{57}Fe probes (C sites) due to a major occupancy of tetrahedral sites by Zn atoms while x is increased. In fact, it was demonstrated in a previous work [22] that the Zn cations occupy the A (tetrahedral) sites on the spinel structure in a higher ratio than for B (octahedral) ones, while x is increased. Likewise, it was detected [23] that Zn substitution of A sites promotes a decrease in A-O-B exchange interaction and, by this way, it was shown that the magnetic moments at B site are no longer rigidly parallel to the few remaining magnetic moments at A site. Then, for these two last samples, we can suggest that their ferromagnetic behaviors are modified by a different magnetic environment of the ^{57}Fe probe, that appears with Zn substitution of A sites.

In the sample with highest content ($x = 1$, zinc ferrite), as it is expected, no sextet was found and this fact is consistent with the presence of Fe^{3+} [24] and the paramagnetic character

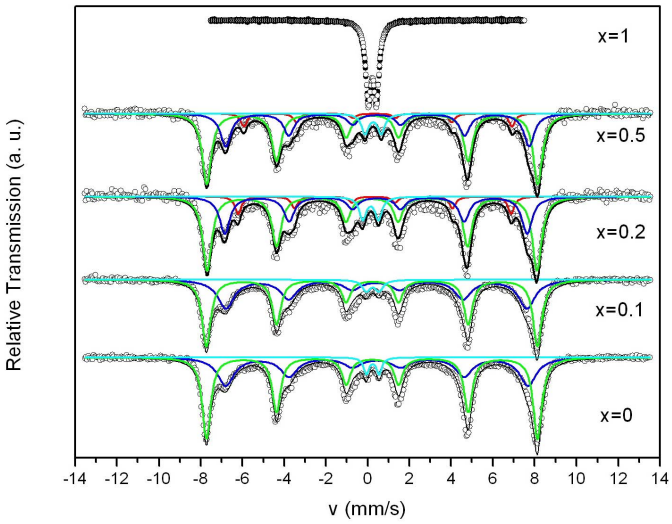

Fig. 3. Relative transmission (dots) with the different fitted hyperfine interactions (color lines) of Mössbauer spectra of Zn-doped magnetite synthesized powders.

TABLE I
HYPERFINE PARAMETERS OBTAINED FROM THE FITTING PROCEDURE OF ^{57}Fe MÖSSBAUER SPECTROSCOPY OF ALL THE SAMPLES: QS STANDS FOR QUADRUPOLAR SHIFT, IS STANDS FOR ISOMER SHIFT, B_{hyp} STANDS FOR THE EFFECTIVE HYPERFINE MAGNETIC FIELD, AND QI STANDS FOR QUADRUPOLAR INTERACTION

Sample		QS (mm/s)	IS (mm/s)	B_{Hyp} (T)	Area (%)
x = 0	A site	-0.017	0.214	49.2	57.8
	B site	0.018	0.434	44.9	38.6
	Q.I.	0.609	0.239	-	3.6
x = 0.1	A site	-0.022	0.211	49.2	53.8
	B site	0.017	0.405	44.7	42.3
	Q.I.	0.610	0.240	-	3.9
x = 0.2	A site	-0.001	0.208	49.0	54.3
	B site	-0.031	0.410	44.9	30.9
	C site	0.052	0.308	40.5	8.6
	Q.I.	0.760	0.140	-	6.2
x = 0.5	A site	-0.006	0.220	49.1	56.8
	B site	0.014	0.007	45.1	30.1
	C site	0.182	0.402	39.8	7.0
	Q.I.	0.760	0.140	-	6.1
x = 1	Q.I.	0.387	0.235	-	100

of this phase. The QI represents a low percentage of iron probes and the corresponding quadrupolar and isomer shifts are different after x value. This last fact is a suggestion that ^{57}Fe is in a different environment in this minority non-magnetic phases.

B. Magnetic Properties

1) DC Magnetic Studies: Hysteresis loops were measured up to ~2400 kA/m at different temperatures (300, 200, 100, 50, and 7 °K). Pure magnetite and doped magnetite up to $x = 0.5$ shows a soft ferromagnetic behavior with a coercive field as low as 5.4 kA/m and squareness ratio ($S = M_r/M_s$) as low as 0.08 (both for sample with $x = 0.2$ at 300 K).

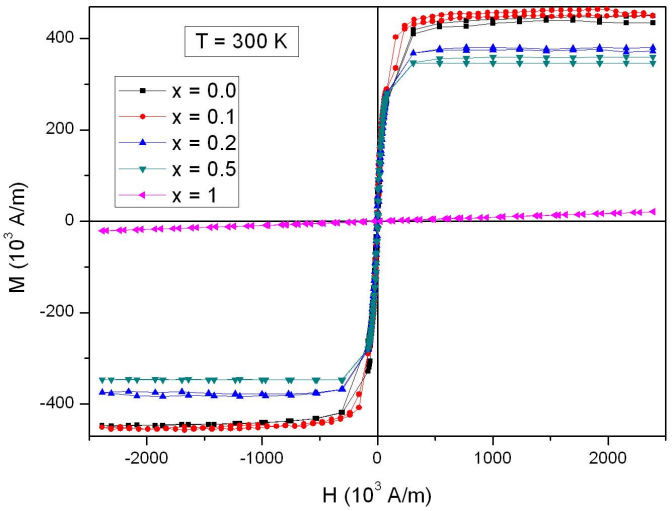

Fig. 4. Hysteresis loops of the different samples obtained measured at RT.

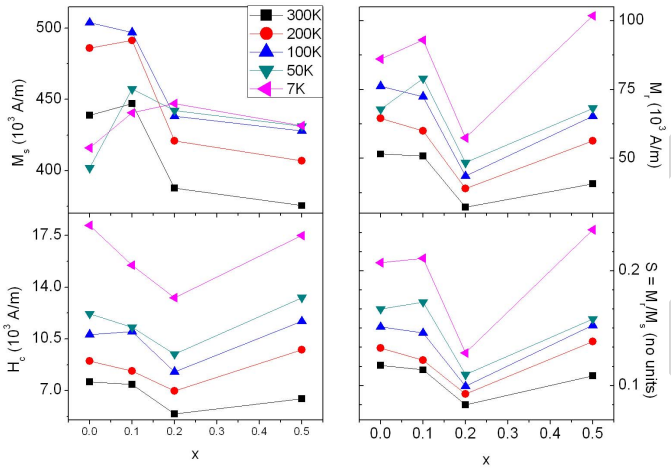

Fig. 5. Evolution of magnetic properties, obtained from hysteresis loops, with Zn fraction (x) and temperature. Counterclockwise: saturation magnetization (M_S), remanence magnetization (Mr), squareness ratio (S), and coercitive field. ■: 300, ●: 200, ▲: 100, ▼: 50, ◀: 7 K.

Meanwhile zinc ferrite ($x = 1$; i.e., Fe_2ZnO_4) shows a paramagnetic behavior as expected. In Fig. 4, we show the hysteresis cycles measured for the samples at 300 K.

A graphical resume of the evolution of the magnetic properties extracted from the hysteresis cycles (saturation M_s, remanence M_r, squareness ratio S, and coercitive field H_c) with the Zn doping fraction (x) and temperature can be seen in Fig. 5. It is clearly shown there that a higher Zn doping fraction modifies the ferrimagnetic properties, giving rise to a maximum in M_s for $x = 0.1$ for temperatures over almost the complete selected range. In addition, the spin canting effect that is present in magnetite and $x = 0.1$ samples occurs at a temperature between 7 and 50 K, as it can be observed from the remanence and saturation behavior with the selected temperatures after Zn concentrations. The increase of M_s with low (up to $x = 0.1$) Zn content can be attributed to a replacement of Fe^{3+} ions by Zn^{2+} causing an enhancement in the resultant of the magnetic moments of Fe ions [25]. Although this increase in M_s must be extended to higher

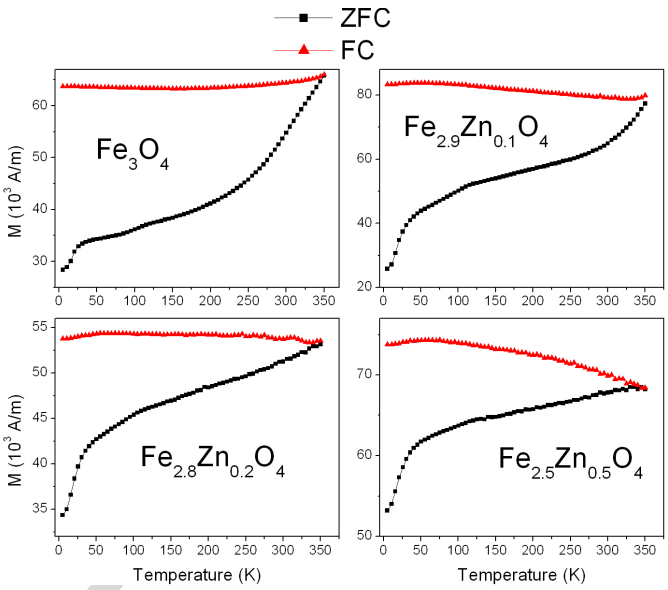

Fig. 6. ZFC-FC curves obtained with an applied field of 50 Oe.

Zn contents up to $x = 0.5$, that was not our case and the reduction of M_s for $x \geq 0.2$ can be attributed to the changes in Fe occupancy of A and B sites (as seen by Mössbauer spectroscopy and also in [8]). We also do not discard effects of size effect and/or effects of interaction between particles. Meanwhile, the sample with 20% of Zn can be tagged as magnetically softest because it has the lowest coercive field. Beside this, it has low values of remanence and squareness ratio.

2) ZFC-FC and AC Susceptibility Measurements: We also have done ZFC-FC measurements with an applied field of 3.98 kA/m. The results can be seen in Fig. 6, which shows thermomagnetic irreversibility ($M_{FC} > M_{ZFC}$) below a certain temperature T_{irr}, which is ~350 K. This reveals that the systems are in a blocked state for all temperatures below the mentioned one. This situation could be explained if it is assumed that our powders act as interacting superparamagnetic systems [26]. The Verwey transition expected for bulk magnetite is not observed in our samples; this can be attributed to the small particle size, as previously observed in [27]. Otherwise, it can be observed that for $x = 0.2$ and 0.5, there is a variation of M versus T behavior for temperatures ~50 K. For this sample, $M(T)$, for both ZFC and FC, a notorious change of concavity is observed. This can be attributed to different exchange interactions of Fe moments after Zn substitution.

We also have measured ac susceptibility from 5 to 300 K applying different field frequencies of 107, 1007, 5007, and 9967 Hz. Results show that imaginary part of susceptibility χ'' has a maximum at a temperature (labeled as T_c), which depends on the used frequency, while real part of susceptibility χ' increases with temperature having an inflection point at the same temperature for which χ'' has its maximum, as it is shown in Fig. 7.

The frequency dependence of T_c taken from the maximum in the curve is in agreement with a thermally activated process for all samples, being well described by the Néel model [28],

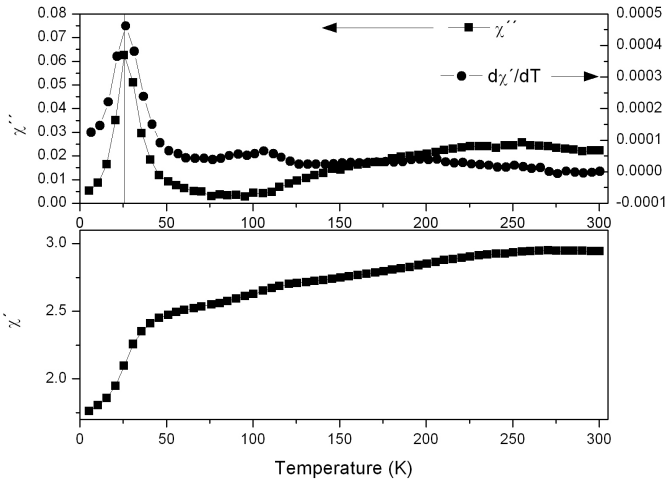

Fig. 7. Real χ' (bottom) and imaginary χ'' part of ac (top) of SI dimensionless susceptibility for undoped magnetite measured at 107 Hz. In the top graph, the derivate of real part with temperature is plotted.

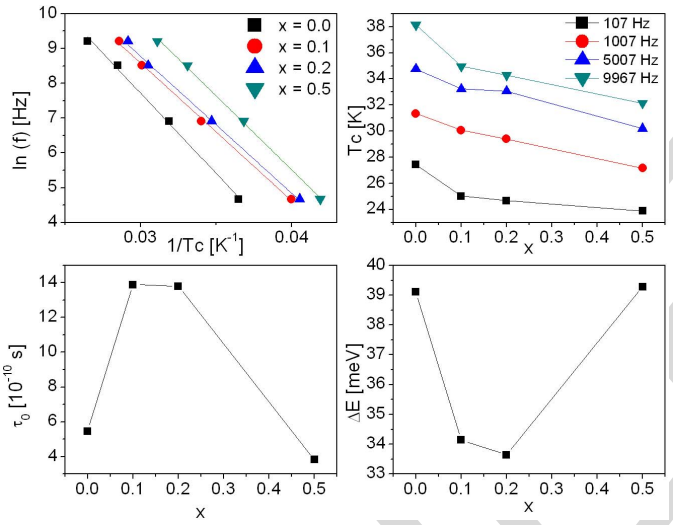

Fig. 8. Arrhenius plots and fits over the frequency versus temperature of maximum (Tc) of χ'' (top–left), evolution of this temperature with the Zn-doping fraction x (top–right), evolution of τ_0 (bottom–left) and ΔE (bottom–right) parameters (obtained from the Arrhenius fits) with Zn-doping fraction x.

as it is shown in Fig. 8. In addition, in Fig. 8, the dependence of the τ_0 and ΔE parameters on the Zn-doping fraction (x) is plotted, as they were obtained by fitting the ($\ln f$) versus ($1/T_c$) data using the Néel–Arrhenius equation

$$\tau = \frac{1}{f} = \tau_0 \cdot e^{\Delta E/(k.\mathrm{Tc})}. \quad (1)$$

The order of magnitude of 10^{-10} s obtained for τ_0 is in agreement with the expected values for this parameter in the Néel model (10^{-9}–10^{-11} s). While for $\Delta E = K_{\mathrm{eff}} \cdot V$ (where K_{eff} is the effective magnetocrystalline anisotropy) has a minimum for $x = 0.2$.

If we consider that, the coercive field at zero temperature is related also with K_{eff} by $H_c(0) = 2K_{\mathrm{eff}}/M_S$ (where M_S is the saturation magnetization) we can see that this matches with the fact that there is a minimum in the coercive field with the Zn content, as it can be observed in Fig. 4.

IV. Conclusion

A study of $Fe_{3-x}Zn_xO_4$, nanoparticles obtained by coprecipitation method, was carried out in order to observe the influence of Zn fraction in their structural and the magnetic properties. These nanoparticles were prepared selecting the Zn doping in the range $0 \leq x \leq 0.5$ and the extreme case of $x = 1$ having a mean crystallite size of 45 nm as it was found by means XRD. According to SEM images the shape of the samples is polihedrical with some spherical shape cases. In the study of magnetic properties at RT, we found the maximum saturation for $x = 0.1$, while the sample with $x = 0.2$ has the minimum coercive field. ZFC-FC curves revealed that the interactions between particles are very strong. The ac magnetic studies show that both imaginary (with a maximum) and real part (with a inflection point) of susceptibility had a critical temperature, which depends on the frequency in a Néel–Arrhenius way. The dependence of the K_{eff} parameter on x fraction, as obtained from fitting the Arrhenius plots, agrees with that obtained from dc magnetization studies.

Acknowledgment

The work of S. Ferrari and F. D. Saccone was supported in part by the National Scientific and Technical Research Council under Project PIP 2009 02122 and in part by the Agencia Nacional de Promoción Científica y Tecnológica under Project PICT 2012 01730. The work of J. C. Aphesteguy was supported by the Universidad de Buenos Aires, Buenos Aires, Argentina, through the UBACyT Research Project under Grant 20020100100325.

References

[1] L. Yu, S. Cao, Y. Liu, J. Wang, C. Jing, and J. Zhang, "Thermal and structural analysis on the nanocrystalline NiCuZn ferrite synthesis in different atmospheres," *J. Magn. Magn. Mater.*, vol. 301, no. 1, pp. 100–107, Jun. 2006.

[2] G. V. Kurlyandskaya, J. Cunanan, S. M. Bhagat, J. C. Aphesteguy, and S. E. Jacobo, "Field-induced microwave absorption in Fe_3O_4 nanoparticles and Fe_3O_4/polyaniline composites synthesized by different methods," *J. Phys. Chem. Sol.*, vol. 68, no. 8, pp. 1527–1532, 2007.

[3] S. Yan, J. Yin, and E. Zhou, "Study on the synthesis of NiZnCu ferrite nanoparticles by PVA sol–gel method and their magnetic properties," *J. Alloys Compounds*, vol. 450, nos. 1–2, pp. 417–420, Feb. 2008.

[4] S. Xuan, F. Wang, Y. Xiang, J. Wang, J. C. Yua, and K. C.-F. Leung, "Facile synthesis of size-controllable monodispersed ferrite nanospheres," *J. Mater. Chem.*, vol. 20, pp. 5086–5094, Mar. 2010.

[5] G. Kurlyandskaya and V. Levit, "Magnetic Dynabeads detection by sensitive element based on giant magnetoimpedance," *Biosensors Bioelectron.*, vol. 20, no. 8, pp. 1611–1616, Feb. 2005.

[6] P. M. Zélis *et al.*, "Structural and magnetic study of zinc-doped magnetite nanoparticles and ferrofluids for hyperthermia applications," *J. Phys. D, Appl. Phys.*, vol. 46, no. 12, pp. 125006-1–125006-12, 2013.

[7] E. Mayes *et al.*, "Biologically derived nanomagnets in self-organized patterned media," *IEEE Trans. Magn.*, vol. 39, no. 2, pp. 623–627, Mar. 2003.

[8] T. F. W. Barth and E. Posnjak, "Spinel structures: With and without variate atom equipoints," *Zeitschrift Kristallographie*, vol. 82, no. 1, pp. 325–341, 1923.

[9] G. Blasse, "Magnetic properties of some oxides with spinel structure," *Philips Res. Rep.*, vol. 20, pp. 528–555, 1965.

[10] B. Behdadfar, A. Kermanpur, H. Sadeghi-Aliabadi, M. del Puerto Morales, and M. Mozaffari, "Synthesis of aqueous ferrofluids of $Zn_xFe_{3-x}O_4$ nanoparticles by citric acid assisted hydrothermal-reduction route for magnetic hyperthermia applications," *J. Magn. Magn. Mater.*, vol. 324, no. 14, pp. 2211–2217, Jul. 2012.

[11] S. Chikazumi, *Physics of Magnetism*. New York, NY, USA: Wiley, 1964.
[12] S. K. Banerjee and W. O'Reilly, "The behaviour of ferrous ions in iron-titanium spinels," *J. Phys. Chem. Solids*, vol. 28, no. 7, pp. 1323–1335, Jul. 1967.
[13] N. M. B. E. Badramany, E. F. Mina, H. D. Merchant, S. Arafa, and R. P. Poplawsky, "Electrical resistivity of magnetite and nickel ferrous ferrite above 300 °K," *J. Amer. Ceram. Soc.*, vol. 62, nos. 3–4, pp. 113–116, Mar. 1979.
[14] D. Venkateshvaran *et al.*, "Epitaxial $Zn_xFe_{3-x}O_4$ thin films: A spintronic material with tunable electrical and magnetic properties," *Phys. Rev. B*, vol. 79, pp. 134405-1–134405-12, Apr. 2009.
[15] K. E. Sickafus, J. M. Wills, and N. W. Grimes, "Structure of spinel," *J. Amer. Ceram. Soc.*, vol. 82, no. 12, pp. 3279–3292, Dec. 1999.
[16] R. R. Shahraki, M. Ebrahimi, S. A. S. Ebrahimi, and S. M. Masoudpanah, "Structural characterization and magnetic properties of superparamagnetic zinc ferrite nanoparticles synthesized by the coprecipitation method," *J. Magn. Magn. Mater.*, vol. 324, no. 22, pp. 3762–3765, Nov. 2012.
[17] R. Sai, S. D. Kulkarni, K. J. Vinoy, N. Bhat, and S. A. Shivashankar, "$ZnFe_2O_4$: Rapid and sub-100 °C synthesis and anneal-tuned magnetic properties," *J. Mater. Chem.*, vol. 22, no. 5, pp. 2149–2156, 2012.
[18] V. Blanco-Gutierrez, E. Climent-Pascual, M. J. Torralvo-Fernandez, R. Saez-Puche, and M. T. Fernandez-Diaz, "Neutron diffraction study and superparamagnetic behavior of $ZnFe_2O_4$ nanoparticles obtained with different conditions," *J. Solid State Chem.*, vol. 184, no. 7, pp. 1608–1613, Jul. 2011.
[19] M. Mozaffari, M. E. Arani, and J. Amighian, "The effect of cation distribution on magnetization of $ZnFe_2O_4$ nanoparticles," *J. Magn. Magn. Mater.*, vol. 322, no. 21, pp. 3240–3244, Nov. 2010.
[20] A. Veiga, M. A. Mayosky, N. Martínez, P. M. Zélis, G. A. Pasquevich, and F. H. Sánchez, "Smooth driving of Mössbauer electromechanical transducers," *Hyperfine Interact.*, vol. 202, nos. 1–3, pp. 107–115, Nov. 2011.
[21] N.-N. Song *et al.*, "Exceeding natural resonance frequency limit of monodisperse Fe_3O_4 nanoparticles via superparamagnetic relaxation," *Nature Sci. Rep.*, vol. 3, pp. 3161-1–3161-55, Nov. 2013.
[22] M. Wen, Q. Li, and Y. Li, "Magnetic, electronic and structural properties of $Zn_xFe_{3-x}O_4$," *J. Electron Spectrosc. Rel. Phenomena*, vol. 153, no. 3, pp. 65–70, Oct. 2006.
[23] Y. Li *et al.*, "Magnetic properties and local structure studies of Zn doped ferrites," *J. Electron Spectrosc. Rel. Phenomena*, vol. 160, nos. 1–3, pp. 1–6, Aug. 2007.
[24] C. N. Chinnasamy, A. Narayanasamy, N. Ponpandian, K. Chattopadhyay, H. Guérault, and J.-M. Greneche, "Magnetic properties of nanostructured ferrimagnetic zinc ferrite," *J. Phys., Condens. Matter*, vol. 12, no. 35, pp. 7795–7805, 2000.
[25] V. A. M. Brabers, *Handbook of Magnetic Materials*, vol. 8, 1997. AQ:14
[26] M. Knobel, W. C. Nunes, L. M. Socolovsky, E. D. Biasi, J. M. Vargas, and J. C. Denardin, "Superparamagnetism and other magnetic features in granular materials: A review on ideal and real systems," *J. Nanosci. Nanotechnol.*, vol. 8, no. 6, pp. 2836–2857, 2008.
[27] G. F. Goya, T. S. Berquó, F. C. Fonseca, and M. P. Morales, "Static and dynamic magnetic properties of spherical magnetite nanoparticles," *J. Appl. Phys.*, vol. 94, no. 5, pp. 3520–3528, 2003.
[28] L. E. F. Néel, "Théorie du traînage magnétique des ferromagnétiques en grains fins avec application aux terres cuites," *Ann. Géophys.*, vol. 5, pp. 99–136, Jan. 1949. AQ:15

AUTHOR QUERIES

AQ:1 = Please provide the zipcode and also confirm the organization name.
AQ:2 = Please provide the expansion for the acronyms "ZFC-FC and "PPMS."
AQ:3 = In line no. 8 "imaginary part have a maximum" changed as "imaginary part has a maximum" as per editing aspect. Please confirm the change.
AQ:4 = Please check whether the edits made in the sentence "To prepare . . ." are OK.
AQ:5 = Please check whether the edits made in the sentence "These differences with. . ." retain the intended meaning.
AQ:6 = Please confirm whether the edits made in the caption of Fig. 2 is appropriate.
AQ:7 = Please check whether the edits made in the sentence "For this sample . . . " retain the intended meaning.
AQ:8 = Please check whether the edits made in the sentence "This can be . . . " retain the intended meaning.
AQ:9 = The phrase "Arrenhius" changed as "Arrhenius" throughout the paper. Please confirm.
AQ:10 = Please check the sentence "While for . . . " for clarity.
AQ:11 = Please check whether the term "polihedrical" should be changed to "polyhedral."
AQ:12 = Please check whether the edits made in the sentence "The ac magnetic studies . . ." retain the intended meaning.
AQ:13 = Please provide the issue no. or month for ref. [9].
AQ:14 = Please provide the publisher name and location for ref. [25].
AQ:15 = Please confirm the article title for ref. [28].

Structural and Magnetic Properties of Zn-Doped Magnetite Nanoparticles Obtained by Wet Chemical Method

Sergio Ferrari, Juan Carlos Aphesteguy, and Fabio Daniel Saccone

Facultad de Ciencias Exactas y Naturales, Instituto de Tecnología y Ciencias de la Ingeniería Ing. Hilario Fernández Long, National Scientific and Technical Research Council, Buenos Aires, Argentina

The structural and magnetic properties of $Fe_{(3-x)}Zn_xO_4$ (x : 0, 0.1, 0.2, 0.5, 1) nanoparticles, prepared by wet chemical method, have been studied by X-ray diffraction (XRD), scanning electron microscopy (SEM), Mössbauer spectroscopy, and magnetization measurements. The nanoparticles are polyhedrical-shaped with a narrow distribution in size as it was verified by SEM. By Rietveld analysis of XRD patterns, it was determined that the crystallites' sizes of $Fe_{(3-x)}Zn_xO_4$ in spinel structure is in the range of 30 to 50 nm. Hysteresis cycles, measured at different temperatures (300, 200, 100, 50, and 7 K), showed an increase in saturation, while temperature is diminished, as it is expected. All the samples, exhibited a high blocking temperature of ∼350 K, as it was determined by ZFC-FC measurements. This fact, reveals their strongly interacting superparamagnetic nature. Real ac susceptibility increases with temperature, while the imaginary part has a maximum, which depends on frequency, and it is related to a critical temperature, which depends on composition. A Néel–Arrhenius dependence of frequency on the critical temperature was found for all the samples. We determined a minimum of the effective anisotropy for $x = 0.2$.

***Index Terms*— Magnetic nanoparticles, Zn-doped magnetite.**

I. Introduction

THE development of nanosized magnetic materials is a subject of considerable interest both for understanding their fundamental properties and for new technological applications because nanoparticles show unusual phenomena compared with bulk or microscale-sized magnets of the same composition [1]–[3].

Several magnetic and mixed metal oxides nanoparticles, having the general formula XY_2O_4, have been investigated because they exhibit interesting and unique physical properties in different areas, such as high density storage [4], color imaging, sensors, biomedical and biological applications [5], [6], spintronic [7], and catalysis.

In these oxidic spinels, the physical properties were found to be dependent on the nature of the involved ions, their charges, and their site distribution among 8-tetrahedral (A) and 16-octahedral (B) sites. Two extreme distributions of cations are possible: 1) the normal $(X)_A[Y_2]_BO_4$ and 2) the inverse $(Y)_A[XY]_BO_4$ distribution [8], where the ions in the octahedral sites are in square brackets. Blasse [9] and Behdadfar *et al.* [10] have studied solid solutions by substituting ions at A and B sites. They have obtained a gradual change in the physical and magnetic properties of these oxidic spinels by varying the composition of the solution.

Magnetite (Fe_3O_4) possesses an inverse spinel structure, where oxygen ions forms an fcc close packing, with a cation distribution after the formula $(Fe^{3+})_A[Fe^{2+}Fe^{3+}]_BO_4$, and is a ferromagnetic oxide with a Curie temperature at 858 K [11]. It has been found [12]–[14] that for substituted magnetite $M_xFe_{3-x}O_4$ (M = Zn, Mn), a fast electron exchange between Fe^{2+} and Fe^{3+} ions on octahedral sites in the spinel lattice is considered as the reason for the higher electrical conductivity in the case of lower values of x. For higher values, other conduction mechanisms should be considered. In addition, doping magnetite with transition elements allows the modification of quantities such as M_S. In addition, ferrimagnetic iron oxides have the largest M_S of all the known biocompatible materials and they are low cost.

Bulk zinc ferrite has a normal spinel structure with the diamagnetic Zn^{2+} ions in the tetrahedral sites and magnetic Fe^{3+} ions in the octahedral sites [15]. Due to antiferromagnetic superexchange interactions between octahedral-coordinated Fe^{3+} ions, bulk zinc ferrite is antiferromagnetic at $T_N = 10$ K. However, scaling to nanometer sizes the magnetic structure of zinc ferrites changes significantly with the redistribution of iron and zinc cations into octahedral and tetrahedral sites. As a result of nanometer scaling, nanocrystalline zinc ferrite shows ferromagnetic behavior. It has been demonstrated that the properties of zinc ferrites are strongly influenced by the composition and microstructure, and can be modified controllably by varying the particle size, processing parameters, and type and concentration of dopant [16]–[18]. Magnetic dilution due to substitution of diamagnetic atoms gives rise to interesting magnetic features in spinel structure compounds.

The aim of this paper is to identify the doping effect of Zn at different concentrations and to analyze its role on modifications of structure, morphology, and magnetic properties of Zn-doped magnetite. Magnetite sample and zinc-substituted samples were obtained by coprecipitation method for its advantage, such as easy preparation, enough digestion to form the final structure suitable, control of particle size, and low cost. We have studied the $Zn_xFe_{3-x}O_4$ system using X-ray diffraction (XRD), scanning electron microscopy (SEM), Mössbauer spectroscopy at room temperature (RT), FC-ZFC measurements, hysteresis loops at different

Manuscript received July 19, 2014; revised September 6, 2014 and October 20, 2014; accepted November 24, 2014. Corresponding author: F. D. Saccone (e-mail: fsaccone@fi.uba.ar).

Color versions of one or more of the figures in this paper are available online at http://ieeexplore.ieee.org.

Digital Object Identifier 10.1109/TMAG.2014.2377132

temperatures, and ac magnetic susceptibility measurements at different frequencies.

II. Experimental

A. Sample Preparation

Fe_3O_4 pure nanoparticles, Zn-doped ferrites according to the formula $Zn_xFe_{3-x}O_4$ with $x = 0.1$, 0.15, 0.2, and 0.5 were prepared by coprecipitation method in aqueous solution of iron sulfate and water mixed with a solution of KNO_3 and NH_3 (more details are given in Section II-A1). $ZnFe_2O_4$ powders were obtained by sol-gel method following a similar procedure employed in [19]. This last method was preferred for this sample, due to its preservation of stoichiometry as it inhibits the Fe^{2+} to Fe^{3+} oxidation.

1) Preparation of Undoped and Doped Magnetite: To prepare the pure and Zn-doped magnetite samples, N_2 was bubbled independently during 20 min through two solutions: 1) Solution 1: 50 mL of concentrated ammonia and KNO_3 (oxidant agent) with a concentration of 2×10^{-2} mol/L were completely dissolved in 540 mL of distilled water at RT and 2) Solution 2: 1.57×10^{-2} mol/L $FeSO_4 \cdot 7H_2O$ was dissolved in 6 mL of H_2SO_4 2M and 54 mL of distilled water at RT. After 20 min, Solution 2 was added slowly under vigorous mechanical stirring and flowing N_2 to Solution 1 at RT. Then the sample was kept at rest inside the reaction vessel at RT during 20 h in order to promote the complete formation of the spinel phase ($pH_{final} \approx 10.0$). The precipitates were separated from the slurry by centrifuging and washed several times with distilled water, methanol and acetone being finally pH $\approx$ 6. As the last step, the nanoparticles were dried in air. For Zn-doped samples $FeSO_4 \cdot 7H_2O$ was partially replaced by $ZnSO_4 \cdot 7H_2O$, in a fraction corresponding to the desired composition.

2) Zinc Ferrite Preparation: In order to prepare Zn ferrite, 0.01 mol $Zn(Ac)_2 \cdot 2H_2O$ and 0.02 mol $Fe(NO_3)_3 \cdot 9H_2O$ were dissolved in 50 mL of distilled water in a reaction vessel and were gelated using 0.1 mol citric acid as a catalyst. The solution was heated at 90 °C with continuous stirring until a highly viscous gel was formed. Then, the resulting gel was dried at 120 °C for 24 h in an oven.

B. Measurement Conditions

XRD was carried out by a Rigaku D/max diffractometer equipped with a vertical goniometer, using a Bragg–Ventano geometry ($\theta - 2\theta$ coupled arms) and Cu-Kα radiation in a $15°-80°$ 2θ range, measuring at every 0.05° step sweeping with a 0.5° per minute velocity. Microscopy images where captured with a Carl Zeiss SMT Supra 40 SEM at 3 kV. The Mössbauer measurements were recorded at RT under transmission geometry with a standard constant acceleration spectrometer, using a 5 mCi ^{57}CoRh radioactive source. Data was recorded using a 1024 channel MDAQ107 data acquisition module [20]. Magnetic properties were measured by a Quantum Design PPMS 9 T, applying a maximum field of 3 T in hysteresis loops. AC susceptibility was measured with frequencies of 107, 1007, 5007, and 9967 Hz applying 238.7 A/m magnetic field amplitude and sweeping temperatures between 5 and 300 K with a step of 5 K.

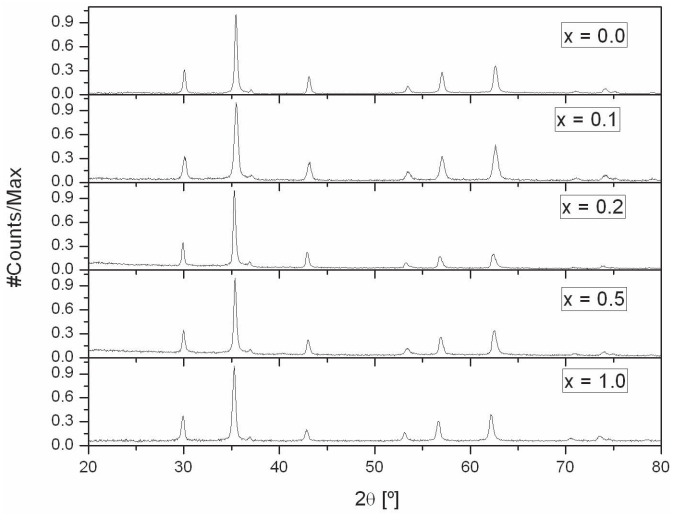

Fig. 1. XRD patterns for the different samples. From top to bottom: increasing zinc content referred in the value of x.

III. Results and Discussion

A. XRD, SEM Images, and Mössbauer Data

All XRD patterns on Fig. 1 shows the typical peaks of magnetite cubic structure (space group Fd3m) with no observation of extra ones which indicate, in principle, that no segregation of other crystalline phases was induced during the synthesis. Then, Zn was incorporated as a dopant, as it was expected. By a Rietveld analysis of the patterns, we estimated the lattice constant between 8.39 and 8.41 Å, and an average grain size in all samples of 45 nm. In details, pure magnetite showed the highest grain size of 55 nm, while for $x = 0.1$ we found the lowest grain size of $\sim$34 nm.

SEM images of synthesized nanoparticles samples with $x = 0$ and $x = 0.1$ are shown in Fig. 2. As it can be seen, the nanoparticles are polyhedrical-shaped with a narrow distribution in size. The observed nanoparticle diameters are larger than the mean grain size as obtained by Rietveld refinement analysis of diffraction patterns. This can be explained from the fact that Rietveld analysis give us information about crystallite sizes rather than the nanoparticle diameter. On the other hand, the mean nanoparticle diameter for $x = 0.1$ is larger than that for $x = 0$. These differences with the results determined by Rietveld analysis for the crystallite size seems to be related to a higher nanoparticles coalescence for $x = 0.1$ than for $x = 0$.

Mössbauer spectroscopy (Fig. 3) showed that partial Zn dilution promotes a higher disorder degree preferentially in the octahedral site (see spectra for samples with $x = 0$, 0.1, 0.2, and 0.5). For $x = 0$ and for $x = 0.1$, we found the evidence of three non-equivalent sites for the ^{57}Fe probe (we fitted its corresponding spectrum with two magnetic sextets, corresponding to tetrahedral sites (A) and octahedral (B) sites, and a quadrupolar interaction (QI). The hyperfine parameters corresponding to octahedral sites (Table I) and its broadened linewidth show that they are occupied by iron probes with a mixed valence between

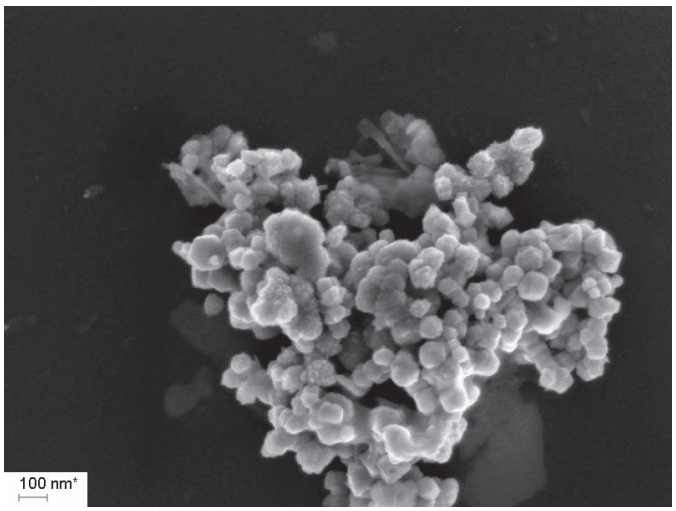

(a)

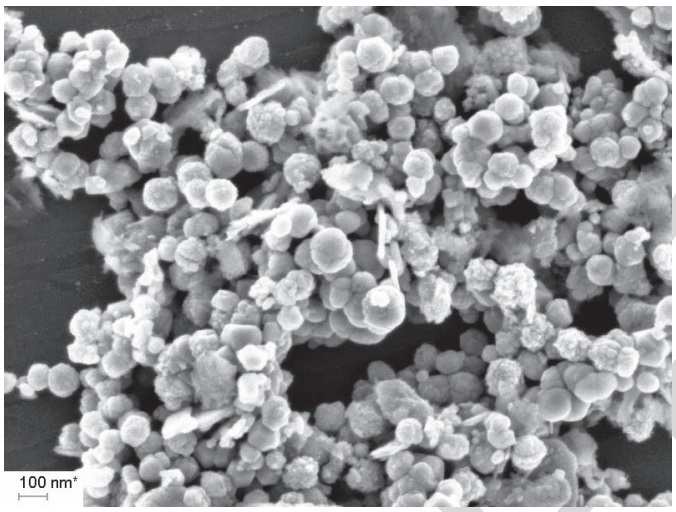

(b)

Fig. 2. SEM images of samples with (a) $x = 0$ and (b) $x = 0.1$.

Fe^{2+} and Fe^{3+} [21]. For the other two above-mentioned concentrations ($x = 0.2$ and $x = 0.5$), it was necessary to add an additional sextet in order to reproduce the presence of a more distorted environment. This additional sextet has a lower hyperfine magnetic field (∼40 T) and is assumed that it shows a different neighborhood for ^{57}Fe probes (C sites) due to a major occupancy of tetrahedral sites by Zn atoms while x is increased. In fact, it was demonstrated in a previous work [22] that the Zn cations occupy the A (tetrahedral) sites on the spinel structure in a higher ratio than for B (octahedral) ones, while x is increased. Likewise, it was detected [23] that Zn substitution of A sites promotes a decrease in A-O-B exchange interaction and, by this way, it was shown that the magnetic moments at B site are no longer rigidly parallel to the few remaining magnetic moments at A site. Then, for these two last samples, we can suggest that their ferromagnetic behaviors are modified by a different magnetic environment of the ^{57}Fe probe, that appears with Zn substitution of A sites.

In the sample with highest content ($x = 1$, zinc ferrite), as it is expected, no sextet was found and this fact is consistent with the presence of Fe^{3+} [24] and the paramagnetic character

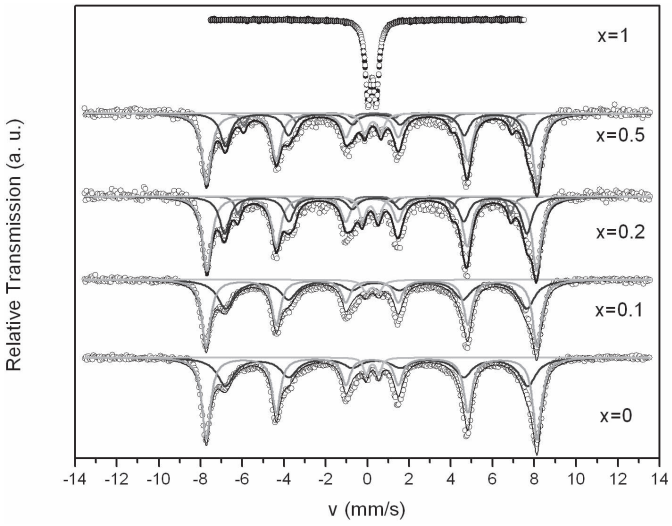

Fig. 3. Relative transmission (dots) with the different fitted hyperfine interactions (color lines) of Mössbauer spectra of Zn-doped magnetite synthesized powders.

TABLE I
HYPERFINE PARAMETERS OBTAINED FROM THE FITTING PROCEDURE OF ^{57}Fe MÖSSBAUER SPECTROSCOPY OF ALL THE SAMPLES: QS STANDS FOR QUADRUPOLAR SHIFT, IS STANDS FOR ISOMER SHIFT, B_{hyp} STANDS FOR THE EFFECTIVE HYPERFINE MAGNETIC FIELD, AND QI STANDS FOR QUADRUPOLAR INTERACTION

Sample		QS (mm/s)	IS (mm/s)	B_{Hyp} (T)	Area (%)
x = 0	A site	-0.017	0.214	49.2	57.8
	B site	0.018	0.434	44.9	38.6
	Q.I.	0.609	0.239	-	3.6
x = 0.1	A site	-0.022	0.211	49.2	53.8
	B site	0.017	0.405	44.7	42.3
	Q.I.	0.610	0.240	-	3.9
x = 0.2	A site	-0.001	0.208	49.0	54.3
	B site	-0.031	0.410	44.9	30.9
	C site	0.052	0.308	40.5	8.6
	Q.I.	0.760	0.140	-	6.2
x = 0.5	A site	-0.006	0.220	49.1	56.8
	B site	0.014	0.007	45.1	30.1
	C site	0.182	0.402	39.8	7.0
	Q.I.	0.760	0.140	-	6.1
x = 1	Q.I.	0.387	0.235	-	100

of this phase. The QI represents a low percentage of iron probes and the corresponding quadrupolar and isomer shifts are different after x value. This last fact is a suggestion that ^{57}Fe is in a different environment in this minority non-magnetic phases.

B. Magnetic Properties

1) DC Magnetic Studies: Hysteresis loops were measured up to ∼2400 kA/m at different temperatures (300, 200, 100, 50, and 7 °K). Pure magnetite and doped magnetite up to $x = 0.5$ shows a soft ferromagnetic behavior with a coercive field as low as 5.4 kA/m and squareness ratio ($S = M_r/M_s$) as low as 0.08 (both for sample with $x = 0.2$ at 300 K).

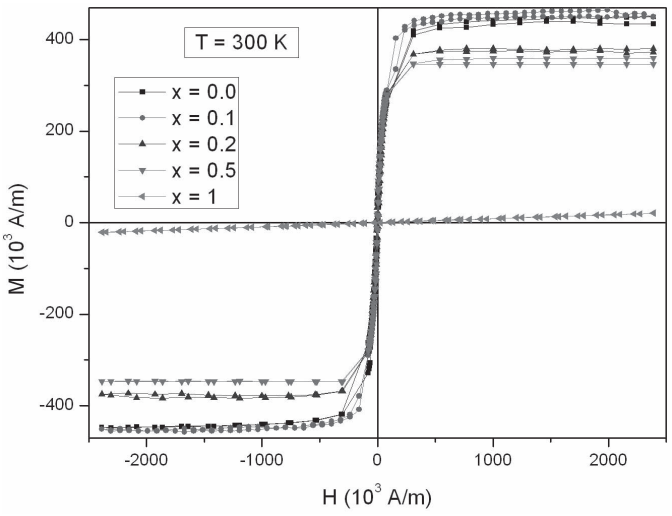

Fig. 4. Hysteresis loops of the different samples obtained measured at RT.

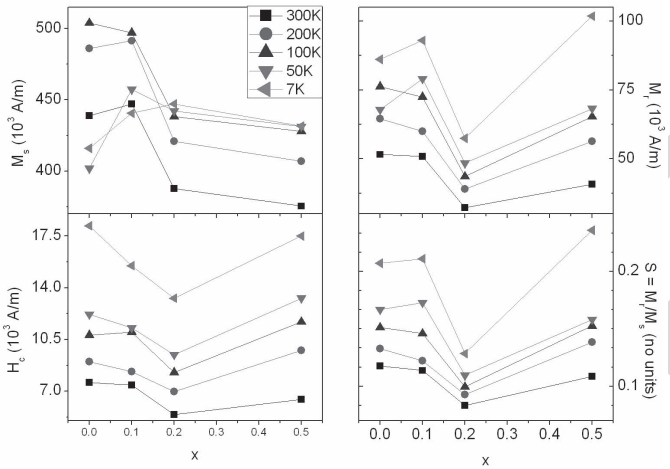

Fig. 5. Evolution of magnetic properties, obtained from hysteresis loops, with Zn fraction (x) and temperature. Counterclockwise: saturation magnetization (M_S), remanence magnetization (Mr), squareness ratio (S), and coercitive field. ■: 300, ●: 200, ▲: 100, ▼: 50, ◀: 7 K.

Meanwhile zinc ferrite ($x = 1$; i.e., Fe_2ZnO_4) shows a paramagnetic behavior as expected. In Fig. 4, we show the hysteresis cycles measured for the samples at 300 K.

A graphical resume of the evolution of the magnetic properties extracted from the hysteresis cycles (saturation M_s, remanence M_r, squareness ratio S, and coercitive field H_c) with the Zn doping fraction (x) and temperature can be seen in Fig. 5. It is clearly shown there that a higher Zn doping fraction modifies the ferrimagnetic properties, giving rise to a maximum in M_s for $x = 0.1$ for temperatures over almost the complete selected range. In addition, the spin canting effect that is present in magnetite and $x = 0.1$ samples occurs at a temperature between 7 and 50 K, as it can be observed from the remanence and saturation behavior with the selected temperatures after Zn concentrations. The increase of M_s with low (up to $x = 0.1$) Zn content can be attributed to a replacement of Fe^{3+} ions by Zn^{2+} causing an enhancement in the resultant of the magnetic moments of Fe ions [25]. Although this increase in M_s must be extended to higher

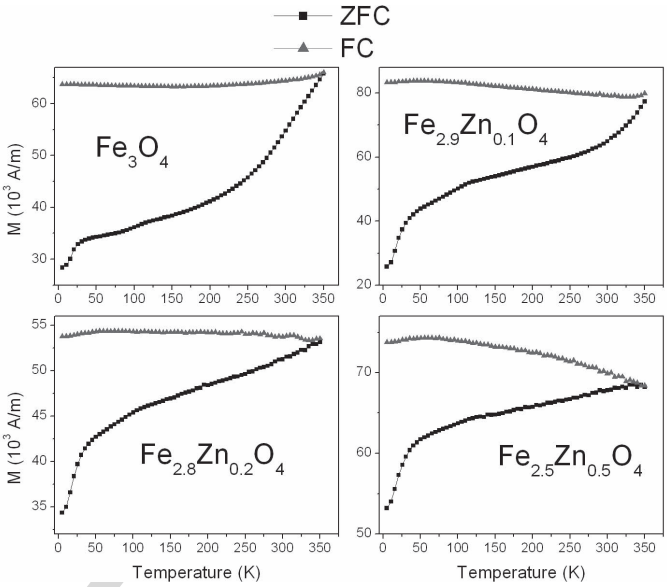

Fig. 6. ZFC-FC curves obtained with an applied field of 50 Oe.

Zn contents up to $x = 0.5$, that was not our case and the reduction of M_s for $x \geq 0.2$ can be attributed to the changes in Fe occupancy of A and B sites (as seen by Mössbauer spectroscopy and also in [8]). We also do not discard effects of size effect and/or effects of interaction between particles. Meanwhile, the sample with 20% of Zn can be tagged as magnetically softest because it has the lowest coercive field. Beside this, it has low values of remanence and squareness ratio.

2) ZFC-FC and AC Susceptibility Measurements: We also have done ZFC-FC measurements with an applied field of 3.98 kA/m. The results can be seen in Fig. 6, which shows thermomagnetic irreversibility ($M_{FC} > M_{ZFC}$) below a certain temperature T_{irr}, which is ∼350 K. This reveals that the systems are in a blocked state for all temperatures below the mentioned one. This situation could be explained if it is assumed that our powders act as interacting superparamagnetic systems [26]. The Verwey transition expected for bulk magnetite is not observed in our samples; this can be attributed to the small particle size, as previously observed in [27]. Otherwise, it can be observed that for $x = 0.2$ and 0.5, there is a variation of M versus T behavior for temperatures ∼50 K. For this sample, $M(T)$, for both ZFC and FC, a notorious change of concavity is observed. This can be attributed to different exchange interactions of Fe moments after Zn substitution.

We also have measured ac susceptibility from 5 to 300 K applying different field frequencies of 107, 1007, 5007, and 9967 Hz. Results show that imaginary part of susceptibility χ'' has a maximum at a temperature (labeled as T_c), which depends on the used frequency, while real part of susceptibility χ' increases with temperature having an inflection point at the same temperature for which χ'' has its maximum, as it is shown in Fig. 7.

The frequency dependence of T_c taken from the maximum in the curve is in agreement with a thermally activated process for all samples, being well described by the Néel model [28],

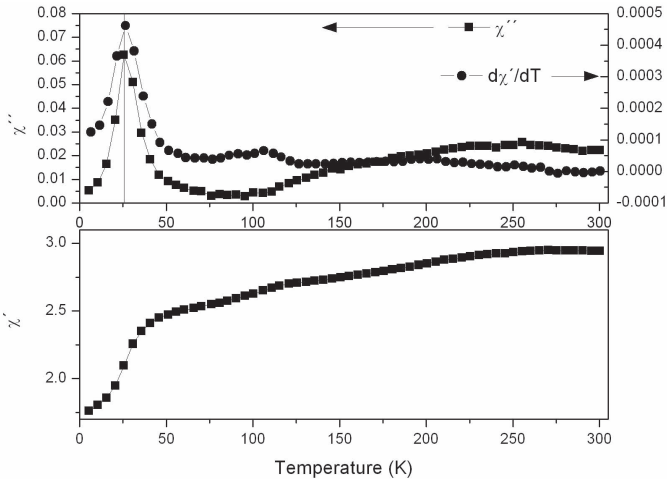

Fig. 7. Real χ' (bottom) and imaginary χ'' part of ac (top) of SI dimensionless susceptibility for undoped magnetite measured at 107 Hz. In the top graph, the derivate of real part with temperature is plotted.

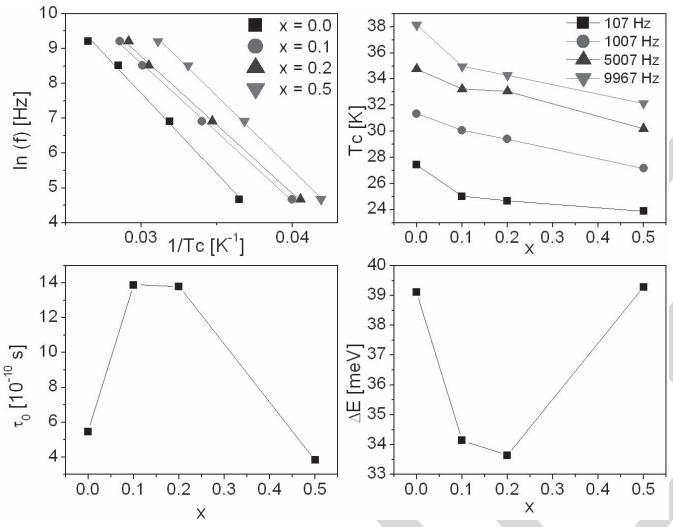

Fig. 8. Arrhenius plots and fits over the frequency versus temperature of maximum (Tc) of χ'' (top–left), evolution of this temperature with the Zn-doping fraction x (top–right), evolution of τ_0 (bottom–left) and ΔE (bottom–right) parameters (obtained from the Arrhenius fits) with Zn-doping fraction x.

as it is shown in Fig. 8. In addition, in Fig. 8, the dependence of the τ_0 and ΔE parameters on the Zn-doping fraction (x) is plotted, as they were obtained by fitting the ($\ln f$) versus ($1/T_c$) data using the Néel–Arrhenius equation

$$\tau = \frac{1}{f} = \tau_0 \cdot e^{\Delta E/(k.\mathrm{Tc})}. \quad (1)$$

The order of magnitude of 10^{-10} s obtained for τ_0 is in agreement with the expected values for this parameter in the Néel model (10^{-9}–10^{-11} s). While for $\Delta E = K_{\mathrm{eff}} \cdot V$ (where K_{eff} is the effective magnetocrystalline anisotropy) has a minimum for $x = 0.2$.

If we consider that, the coercive field at zero temperature is related also with K_{eff} by $H_c(0) = 2K_{\mathrm{eff}}/M_S$ (where M_S is the saturation magnetization) we can see that this matches with the fact that there is a minimum in the coercive field with the Zn content, as it can be observed in Fig. 4.

IV. Conclusion

A study of $Fe_{3-x}Zn_xO_4$, nanoparticles obtained by coprecipitation method, was carried out in order to observe the influence of Zn fraction in their structural and the magnetic properties. These nanoparticles were prepared selecting the Zn doping in the range $0 \leq x \leq 0.5$ and the extreme case of $x = 1$ having a mean crystallite size of 45 nm as it was found by means XRD. According to SEM images the shape of the samples is polihedrical with some spherical shape cases. In the study of magnetic properties at RT, we found the maximum saturation for $x = 0.1$, while the sample with $x = 0.2$ has the minimum coercive field. ZFC-FC curves revealed that the interactions between particles are very strong. The ac magnetic studies show that both imaginary (with a maximum) and real part (with a inflection point) of susceptibility had a critical temperature, which depends on the frequency in a Néel–Arrhenius way. The dependence of the K_{eff} parameter on x fraction, as obtained from fitting the Arrhenius plots, agrees with that obtained from dc magnetization studies.

Acknowledgment

The work of S. Ferrari and F. D. Saccone was supported in part by the National Scientific and Technical Research Council under Project PIP 2009 02122 and in part by the Agencia Nacional de Promoción Científica y Tecnológica under Project PICT 2012 01730. The work of J. C. Aphesteguy was supported by the Universidad de Buenos Aires, Buenos Aires, Argentina, through the UBACyT Research Project under Grant 20020100100325.

References

[1] L. Yu, S. Cao, Y. Liu, J. Wang, C. Jing, and J. Zhang, "Thermal and structural analysis on the nanocrystalline NiCuZn ferrite synthesis in different atmospheres," *J. Magn. Magn. Mater.*, vol. 301, no. 1, pp. 100–107, Jun. 2006.

[2] G. V. Kurlyandskaya, J. Cunanan, S. M. Bhagat, J. C. Aphesteguy, and S. E. Jacobo, "Field-induced microwave absorption in Fe_3O_4 nanoparticles and Fe_3O_4/polyaniline composites synthesized by different methods," *J. Phys. Chem. Sol.*, vol. 68, no. 8, pp. 1527–1532, 2007.

[3] S. Yan, J. Yin, and E. Zhou, "Study on the synthesis of NiZnCu ferrite nanoparticles by PVA sol–gel method and their magnetic properties," *J. Alloys Compounds*, vol. 450, nos. 1–2, pp. 417–420, Feb. 2008.

[4] S. Xuan, F. Wang, Y. Xiang, J. Wang, J. C. Yua, and K. C.-F. Leung, "Facile synthesis of size-controllable monodispersed ferrite nanospheres," *J. Mater. Chem.*, vol. 20, pp. 5086–5094, Mar. 2010.

[5] G. Kurlyandskaya and V. Levit, "Magnetic Dynabeads detection by sensitive element based on giant magnetoimpedance," *Biosensors Bioelectron.*, vol. 20, no. 8, pp. 1611–1616, Feb. 2005.

[6] P. M. Zélis *et al.*, "Structural and magnetic study of zinc-doped magnetite nanoparticles and ferrofluids for hyperthermia applications," *J. Phys. D, Appl. Phys.*, vol. 46, no. 12, pp. 125006-1–125006-12, 2013.

[7] E. Mayes *et al.*, "Biologically derived nanomagnets in self-organized patterned media," *IEEE Trans. Magn.*, vol. 39, no. 2, pp. 623–627, Mar. 2003.

[8] T. F. W. Barth and E. Posnjak, "Spinel structures: With and without variate atom equipoints," *Zeitschrift Kristallographie*, vol. 82, no. 1, pp. 325–341, 1923.

[9] G. Blasse, "Magnetic properties of some oxides with spinel structure," *Philips Res. Rep.*, vol. 20, pp. 528–555, 1965.

[10] B. Behdadfar, A. Kermanpur, H. Sadeghi-Aliabadi, M. del Puerto Morales, and M. Mozaffari, "Synthesis of aqueous ferrofluids of $Zn_xFe_{3-x}O_4$ nanoparticles by citric acid assisted hydrothermal-reduction route for magnetic hyperthermia applications," *J. Magn. Magn. Mater.*, vol. 324, no. 14, pp. 2211–2217, Jul. 2012.

[11] S. Chikazumi, *Physics of Magnetism*. New York, NY, USA: Wiley, 1964.
[12] S. K. Banerjee and W. O'Reilly, "The behaviour of ferrous ions in iron-titanium spinels," *J. Phys. Chem. Solids*, vol. 28, no. 7, pp. 1323–1335, Jul. 1967.
[13] N. M. B. E. Badramany, E. F. Mina, H. D. Merchant, S. Arafa, and R. P. Poplawsky, "Electrical resistivity of magnetite and nickel ferrous ferrite above 300 °K," *J. Amer. Ceram. Soc.*, vol. 62, nos. 3–4, pp. 113–116, Mar. 1979.
[14] D. Venkateshvaran *et al.*, "Epitaxial $Zn_xFe_{3-x}O_4$ thin films: A spintronic material with tunable electrical and magnetic properties," *Phys. Rev. B*, vol. 79, pp. 134405-1–134405-12, Apr. 2009.
[15] K. E. Sickafus, J. M. Wills, and N. W. Grimes, "Structure of spinel," *J. Amer. Ceram. Soc.*, vol. 82, no. 12, pp. 3279–3292, Dec. 1999.
[16] R. R. Shahraki, M. Ebrahimi, S. A. S. Ebrahimi, and S. M. Masoudpanah, "Structural characterization and magnetic properties of superparamagnetic zinc ferrite nanoparticles synthesized by the coprecipitation method," *J. Magn. Magn. Mater.*, vol. 324, no. 22, pp. 3762–3765, Nov. 2012.
[17] R. Sai, S. D. Kulkarni, K. J. Vinoy, N. Bhat, and S. A. Shivashankar, "$ZnFe_2O_4$: Rapid and sub-100 °C synthesis and anneal-tuned magnetic properties," *J. Mater. Chem.*, vol. 22, no. 5, pp. 2149–2156, 2012.
[18] V. Blanco-Gutierrez, E. Climent-Pascual, M. J. Torralvo-Fernandez, R. Saez-Puche, and M. T. Fernandez-Diaz, "Neutron diffraction study and superparamagnetic behavior of $ZnFe_2O_4$ nanoparticles obtained with different conditions," *J. Solid State Chem.*, vol. 184, no. 7, pp. 1608–1613, Jul. 2011.
[19] M. Mozaffari, M. E. Arani, and J. Amighian, "The effect of cation distribution on magnetization of $ZnFe_2O_4$ nanoparticles," *J. Magn. Magn. Mater.*, vol. 322, no. 21, pp. 3240–3244, Nov. 2010.
[20] A. Veiga, M. A. Mayosky, N. Martínez, P. M. Zélis, G. A. Pasquevich, and F. H. Sánchez, "Smooth driving of Mössbauer electromechanical transducers," *Hyperfine Interact.*, vol. 202, nos. 1–3, pp. 107–115, Nov. 2011.
[21] N.-N. Song *et al.*, "Exceeding natural resonance frequency limit of monodisperse Fe_3O_4 nanoparticles via superparamagnetic relaxation," *Nature Sci. Rep.*, vol. 3, pp. 3161-1–3161-55, Nov. 2013.
[22] M. Wen, Q. Li, and Y. Li, "Magnetic, electronic and structural properties of $Zn_xFe_{3-x}O_4$," *J. Electron Spectrosc. Rel. Phenomena*, vol. 153, no. 3, pp. 65–70, Oct. 2006.
[23] Y. Li *et al.*, "Magnetic properties and local structure studies of Zn doped ferrites," *J. Electron Spectrosc. Rel. Phenomena*, vol. 160, nos. 1–3, pp. 1–6, Aug. 2007.
[24] C. N. Chinnasamy, A. Narayanasamy, N. Ponpandian, K. Chattopadhyay, H. Guérault, and J.-M. Greneche, "Magnetic properties of nanostructured ferrimagnetic zinc ferrite," *J. Phys., Condens. Matter*, vol. 12, no. 35, pp. 7795–7805, 2000.
[25] V. A. M. Brabers, *Handbook of Magnetic Materials*, vol. 8, 1997. AQ:14
[26] M. Knobel, W. C. Nunes, L. M. Socolovsky, E. D. Biasi, J. M. Vargas, and J. C. Denardin, "Superparamagnetism and other magnetic features in granular materials: A review on ideal and real systems," *J. Nanosci. Nanotechnol.*, vol. 8, no. 6, pp. 2836–2857, 2008.
[27] G. F. Goya, T. S. Berquó, F. C. Fonseca, and M. P. Morales, "Static and dynamic magnetic properties of spherical magnetite nanoparticles," *J. Appl. Phys.*, vol. 94, no. 5, pp. 3520–3528, 2003.
[28] L. E. F. Néel, "Théorie du traînage magnétique des ferromagnétiques en grains fins avec application aux terres cuites," *Ann. Géophys.*, vol. 5, pp. 99–136, Jan. 1949. AQ:15

AUTHOR QUERIES

AQ:1 = Please provide the zipcode and also confirm the organization name.
AQ:2 = Please provide the expansion for the acronyms "ZFC-FC and "PPMS."
AQ:3 = In line no. 8 "imaginary part have a maximum" changed as "imaginary part has a maximum" as per editing aspect. Please confirm the change.
AQ:4 = Please check whether the edits made in the sentence "To prepare . . ." are OK.
AQ:5 = Please check whether the edits made in the sentence "These differences with. . ." retain the intended meaning.
AQ:6 = Please confirm whether the edits made in the caption of Fig. 2 is appropriate.
AQ:7 = Please check whether the edits made in the sentence "For this sample . . . " retain the intended meaning.
AQ:8 = Please check whether the edits made in the sentence "This can be . . . " retain the intended meaning.
AQ:9 = The phrase "Arrenhius" changed as "Arrhenius" throughout the paper. Please confirm.
AQ:10 = Please check the sentence "While for . . . " for clarity.
AQ:11 = Please check whether the term "polihedrical" should be changed to "polyhedral."
AQ:12 = Please check whether the edits made in the sentence "The ac magnetic studies . . ." retain the intended meaning.
AQ:13 = Please provide the issue no. or month for ref. [9].
AQ:14 = Please provide the publisher name and location for ref. [25].
AQ:15 = Please confirm the article title for ref. [28].